VTT Technical Research Centre of Finland

Clay Composites by In Situ Polymerization of Ionic Liquid-Based Dispersions

Salminen, Linda; Karjalainen, Erno; Aseyev, Vladimir o.; Tenhu, Heikki

Link to publication

Article

Clay Composites by *In Situ* Polymerization of Ionic Liquid-Based Dispersions

Linda Salminen, Erno Karjalainen,* Vladimir O. Aseyev,* and Heikki Tenhu

Cite This: https://doi.org/10.1021/acsapm.3c00601

Read Online

ACCESS | Metrics & More | Article Recommendations | SI Supporting Information

ABSTRACT: Flexible composite materials were prepared by *in situ* copolymerization of ionic liquid like monomers—namely 1-vinyl-3-ethyl imidazolium bis(trifluoromethane)sulfonimide (M1) and 1-(2-acryloyloxyundecyl)-3-methylimidazolium bis(trifluoromethane)sulfonimide (M2) that were cross-linked with 1,1′-octane-1,8-diylbis(3-vinyl imidazolium) di[bis(trifluoromethane)sulfonimide] (CL). Mixtures of polymerizable ionic liquids were used to disperse organo-modified montmorillonite clay as a filler. Polymerization of the mixtures resulted in copolymer composites. The glass transition temperature of the composites could be tuned in the range of −2−127 °C by varying the ratio of the ionic liquid monomers M1 and M2, which is presented in the article for the first time along with its homopolymer. The mechanical properties were significantly enhanced by using a copolymer matrix instead of either of the respective homopolymers. The toughest M1−M2 copolymer composite exhibited a toughness of 5.3 ± 1.4 MPa, while the toughnesses of corresponding poly(M1) and poly(M2) films were 0.6 ± 0.2 and 0.5 ± 0.003 MPa, respectively. The composite could be filled uniformly with large amounts of montmorillonite clay. The copolymer matrix was able to take up large amounts of clay while still exhibiting mechanical properties that surpassed the unfilled matrix.

KEYWORDS: *Composites, Mechanical properties, Particle-reinforcement, Poly(ionic liquids), Materials*
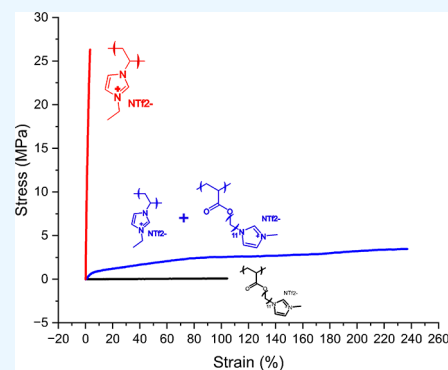
1. INTRODUCTION

Poly(ionic liquids), or polymerized ionic liquids (PIL), are polymerization products of polymerizable ionic liquids (IL).[1,2] The properties of PILs can change drastically depending on the choice of counterion. For instance, glass transition temperature (T_g), thermal stability, mechanical strength, electrical properties, and solubility can be effectively tuned by the choice of the counterion.[3−11] Bis(trifluoromethane)sulfonimide (NTf_2), which is utilized in this work, is known for its ability to turn ILs and PILs essentially water-insoluble.[12] NTf_2 also provides ILs and PILs with relatively low melting points and T_gs, respectively.[3]

PILs combine the benefits of ionic liquid-like tunability and solid form that enhances their moldability. PILs also exhibit ionic conductivity and thus PILs have been studied extensively for applications as electrolytes.[13] However, pure PIL membranes are often brittle.[14−20] The properties of PILs, such as mechanical strength can be improved by preparing PILs in the form of composites. One example of this is the preparation of composites of PILs and free ILs.[21] The composites tend to exhibit better mechanical properties than plain PILs due to the plasticizing effect of IL.

Polymers have commonly been reinforced with particulate materials. For example, biobased fillers such as cellulose have been used to strengthen PILs. Grygiel et al.[22] used PIL-functionalized cellulose nanofibrils for PIL membrane reinforcement, and observed substantial improvements in mechanical properties of the membranes with 5 wt % filler loading. Vilela et al.[23] prepared nanocomposite membranes consisting of bacterial nanocellulose and PIL, in which the bacterial cellulose content was varied from 29 wt % to 85 wt %. Increasing the bacterial cellulose content increased both the tensile modulus and strength of the composites.

Inorganic materials are another group of commonly utilized reinforcing fillers. Carbon nanomaterials, for instance, are popular fillers that have been used with PILs also. Fukushima et al.[24] have prepared PIL-carbon nanotube composites and observed a 120-fold enhancement in the tensile modulus with 7 wt % filler loading. Wang et al.[25] used Al_2O_3 nanoparticles in PIL-based gel polymer electrolytes, and the filler enhanced the mechanical stability of the materials. Likewise, Fdz de Anastro et al.[26] opted for Al_2O_3 as the filler material for their PIL-based composite. The storage modulus was seen to improve with 5 wt % filler loading.

A

In this work, PILs are reinforced with montmorillonite clay. Montmorillonite clay (MMT) is a layered aluminosilicate in which negatively charged alumina and silica layers are compensated by small cations such as Na^+ or Ca^{2+}. As the montmorillonite layers are charged, ionic species, such as ILs and PILs may present strong interactions with the clay layers.[27] Montmorillonite clay is one of the most commonly used reinforcing fillers. It is versatile as its hydrophilicity can be readily tuned with simple anion exchanges. Exchanging the hydrated interlayer cations with organic ones turns the clay's surface more organophilic. This extends montmorillonite clay's applicability also to more hydrophobic media. Such cation-exchanged clays—organoclays—have been used as reinforcing fillers in polymer composites[28,29] However, their utilization with PILs has been less common.[11,30−32]

Copolymerization offers a straightforward way to adjust polymer properties.[33] For instance, brittleness is related to the material's glass transition temperature.[34] Softer, more resilient materials can be obtained by combining a high T_g polymer with one that has a lower T_g. The physicochemical properties of PILs are strongly dependent on the constituent cations and anions.[35] The anion-dependence in particular is known to be significant. Larger anions can hinder ionic associations and thus lower the PIL's T_g.[3] Different aspects of the cations, such as the alkyl substituent length can also influence the T_g. Shorter alkyl substituents are less mobile and give lower T_g values.[36]

Ionic liquids are particularly well-known as powerful solvents. Therefore, our interest has been in employing polymerizable ionic liquids as combined dispersants and matrix constituents in composite materials. We already reported the preparation of glassy, clay-filled composites and the present contribution continues the work by diversifying the material properties through copolymerization.[11]

This article presents composite materials based solely on copolymerization of ionic monomers. First, the properties of copolymers of two IL monomers in various ratios are presented. Then the IL monomer ratio that provided the toughest materials was used in composites with different filler loadings. The composites were filled with organically modified montmorillonite clay (OMMT). The article focuses especially on the effect of filler content on mechanical properties.

2. EXPERIMENTAL PART

2.1. Materials. 1-Vinylimidazole (Aldrich, > 99%) was passed through a basic aluminum oxide column and filtered. AIBN (Aldrich, 98%) was recrystallized from methanol. Butyl acrylate was distilled under vacuum and stored in a freezer. Bromoethane (Aldrich, 98%), 1,8-dibromooctane (Aldrich, 98%), diphenyl(2,4,6-trimethylbenzoyl)-phosphine oxide (TMDPO) (Aldrich, 97%), 11-bromoundecanol (Alrich, 89%), 1-methylimidazole (Aldrich), acryloyl chloride (Aldrich), ammonium peroxydisulfate (APS) (Aldrich, 98%), triethyl-amine (Merck), 3,4-ethylenedioxythiophene (EDOT) (Aldrich, 99%), bis(trifluoromethane)sulfonimide lithium salt (LiNTf$_2$) (Aldrich, >99%), and montmorillonite clay (MMT) (Aldrich, K10) were used as received.

2.2. Syntheses. *1-Vinyl-3-ethyl imidazolium Bromide (VEImBr).* A mixture of 1-vinylimidazole (15.01 g, 159 mmol) and bromoethane (52.30 g, 480 mmol) was purged with nitrogen for 15 min. The mixture was reacted at 40 °C for 46 h. The solidified reaction mixture was precipitated twice from chloroform to ethyl acetate. The product was dried at room temperature under vacuum (4 h, <2 mbar), and the product was obtained in the form of a white powder. The yield was 93.7%. The product's NMR spectrum is given in Figure S1A, and the IR spectrum is in Figure S2A. ^{1}HNMR (500 MHz, D2O, δ, ppm):

8.98 (s, 1H), 7.70 (s, 1H), 7.53 (s, 1H), 7.07 (dd, 1H), 5.73 (dd, 1H), 5.35 (dd, 1H), 4.21 (q, 2H), 1.46 (t, 3H). IR (ν): 3419 (m), 3132 (w), 3059 (s), 2991 (w), 2835 (w), 1659 (s), 1582 (s), 1545 (s), 1458 (m), 1375 (m), 1331 (m), 1304 (m), 1258 (m), 1184 (s), 1167 (s), 1047 (w), 977 (s), 926 (s), 854 (s), 781 (s), 716 (w), 691 (m).

1-Vinyl-3-ethyl Imidazolium Bis(trifluoromethane)sulfonimide (M1). LiNTf$_2$ (23.33 g, 81.3 mmol) was dissolved in 20 mL of water and added dropwise into a vigorously stirred solution of VEImBr (15.07 g, 74.2 mmol) in 20 mL of dichloromethane. Sixteen hours later, the phases were separated and the aqueous phase was extracted with dichloromethane (2 × 30 mL). The combined organic phases were washed with water (3 × 100 mL) and dried over 3 Å molecular sieves. Dichloromethane was evaporated, and the product was further dried at room temperature under <2 mbar vacuum for 3 h. The yield was 99.5%, and the product was a pale, yellowish oil. Purity of the product was verified with ^{1}H NMR, and the spectrum is available in Figure S1B. 1HNMR (500 MHz, acetone-D6, δ, ppm): 9.37 (s, 1H), 8.14 (s. 1H), 7.94 (s, 1H), 7.40 (dd, 1H), 6.03 (dd, 1H), 5.51 (dd, 1H), 4.49 (q, 2H), 1.64 (t, 3H). IR (ν): 3153 (m), 3108 (w), 2994 (w), 2953 (w), 2924 (w), 1659 (m), 1573 (m), 1554 (m), 1471 (w), 1455 (w), 1347 (s), 1329 (s), 1179 (s), 1133 (s), 1052 (s), 954 (m), 918 (m), 844 (m), 790 (m), 763 (s), 739 (s), 702 (w), 686 (w).

1,1′-Octane-1,8-diylbis(3-vinyl imidazolium) Di[bis-(trifluoromethane)sulfonimide] (CL). This work utilizes the same cross-linker that we have reported earlier.[11] For convenience of the reader, the synthesis is summarized herein. A mixture of 1-vinylimidazole (17.30 g, 183.9 mmol) and 1,8-dibromooctane (5.01 g, 18.4 mmol) was purged with nitrogen for 40 min. After reacting the mixture for 18 h at 40 °C, the product was precipitated into ethyl acetate. The obtained precipitate was dissolved in water, and the solution was washed with dichloromethane (3 × 100 mL). After washing, the solution was added into aqueous LiNTf$_2$ (12.68 g, 44.2 mmol LiNTf$_2$ in 200 mL of water) under vigorous stirring. The resulting precipitate was filtered out and dissolved in dichloro-methane. The solution was washed with water (3 × 100 mL) and dried over 3 Å molecular sieves. Dichloromethane was evaporated, and the resulting white solid was dried at room temperature under vacuum (3 h, <2 mbar) (80.6% yield). The NMR spectrum of the product is given in Figure S3. ^{1}HNMR (500 MHz, acetone-d6, δ, ppm): 9.37 (s, 2H), 8.16 (s, 2H), 7.93 (s, 2H), 6.02 (dd, 2H), 5.52 (dd, 2H), 4.44 (t, 4H), 2.03 (m, 4H), 1.42 (t, 8H). IR (ν): 3676 (w), 3661 (w), 3146 (m), 3125 (w), 3098 (w), 3078 (w), 2988 (m), 2970 (m), 2936 (m), 2901 (m), 2870 (m), 1655 (w), 1574 (m), 1551 (m), 1458 (w), 1348 (s), 1240 (m), 1177 (s), 1134 (s), 1049 (s), 957 (m), 926 (m), 868 (w), 845 (m), 793 (m), 762 (m), 739 (m), 681 (w).

Organoclay (OMMT). Montmorillonite clay (8.01 g) was dispersed in 150 mL of water. VEImBr (3.25 g, 16 mmol) in 20 mL of water was added to the clay dispersion. After stirring for 21 h at room temperature, the product was washed with water. Washing was repeated until the AgNO$_3$ test no longer indicated the presence of halide anions in washing water. The organically modified clay was dried for 5 h at 50 °C under vacuum (<2 mbar) (7.64 g yield).

11-Bromoundecyl Acrylate. 11-Bromoundecyl acrylate was synthesized according to a procedure from the literature.[37] 11-Bromoundecanol (25.89 g, 103.1 mmol) was dissolved in 100 mL of tetrahydrofuran (THF), and the solution was cooled down in an ice bath. Triethylamine (13.57 g, 134.1 mmol) in 100 mL of THF was added to the cold solution upon stirring. The mixture was purged with nitrogen for 10 min and acryloyl chloride (12.18 g, 134.6 mmol), dissolved in 100 mL of THF was added slowly to the reaction mixture under nitrogen atmosphere. The mixture was stirred for 4 days at room temperature. Then the mixture was filtered, and the filtrate was washed with 2% NaHCO$_3$ and dried over 3 Å molecular sieves. The product was then passed through Al$_2$O$_3$ with dichloromethane. The yellowish, liquid product was isolated by evaporating the solvent (17.55 g, 55.8% yield). ^{1}HNMR spectrum is available as Figure S4 in SI. ^{1}HNMR (500 MHz, CDCl3, δ, ppm): 6.40 (m, 1H), 6.13 (m, 1H), 5.82 (m, 1H), 4.15 (t, 2H), 3.41 (t, 2H), 1.86 (m, 2H), 1.67 (m, 2H), 1.43−1.29 (m, 14H). IR (ν): 3042 (w), 2926 (m), 2855 (m),

1722 (s), 1636 (w), 1620 (w), 1466 (w), 1406 (m), 1294 (m), 1271(m), 1186 (s), 1061 (m), 984 (m), 966 (m), 810 (m), 721 (w), 646 (w).

1-(2-Acryloyloxyundecyl)-3-methylimidazolium Bromide (M2-Br). A mixture of 11-bromoundecyl acrylate (20.01 g, 65.6 mmol), 1-methylimidazole (6.46 g, 78.7 mmol), and a small amount of inhibitor (2,6-di*tert*-butyl-4-methylphenol) was purged with nitrogen for 20 min and stirred at 40 °C for 42 h. The product was precipitated in diethyl ether (21.34 g, 84.0% yield). The product was a white, waxy solid. The IR spectrum of the product is given in Figure S2B, and the NMR spectrum is in Figure S5A. ^{1}HNMR (500 MHz, CDCl3, δ, ppm): 10.58 (s, 1H), 7.42 (s, 1H), 7.32 (s, 1H), 6,41 (m, 1H), 6.13 (m, 1H), 5.83 (m, 1H), 4.33 (m, 2H), 4.17−4.15 (m, 5H), 1.92 (m, 4H), 1.67 (m, 2H), 1.40−1.25 (m, 14H). IR (ν): 3389 (m), 3237 (w), 3148 (w), 3102 (m), 3061 (m), 2953 (w), 2916 (s), 2853 (m), 2112 (w), 2070 (w), 2016 (w), 1728 (s), 1630 (m), 1574 (m), 1477 (m), 1470 (m), 1412 (s), 1385 (m), 1341 (m), 1300 (s), 1184 (s), 1171 (s), 1090 (w), 1053 (m), 1030 (m), 1009 (m), 995 (m), 970 (m), 891 (w), 858 (w), 820 (m), 812 (m), 781 (m), 739 (w), 729 (w), 719 (w), 679 (w), 662 (w).

1-(2-Acryloyloxyundecyl)-3-methylimidazolium Bis-(trifluoromethane)sulfonimide (M2). To the best of the authors' knowledge, M2 is synthesized for the first time herein. M2-Br (15.00 g, 38.7 mmol) was dissolved in 20 mL of dichloromethane, and LiNTf2 (12.23 g, 42.6 mmol) was dissolved in 20 mL of water. The LiNTf2 solution was added dropwise into the vigorously stirred M2-Br solution. The mixture was stirred 19 h at room temperature, and the phases were separated. The aqueous phase was extracted with dichloromethane (2 × 30 mL). The combined organic phases were washed with water (3 × 100 mL) and dried over 3 Å molecular sieves. The solvent was evaporated, yielding a pale liquid (19.66 g, 86.4% yield). The NMR spectrum of the product is given in Figure S5B, and the IR spectrum is in Figure S2B. 1HNMR (500 MHz, CDCl3, δ, ppm): 8.78 (s, 1H), 7.34 (t, 1H), 7.31 (t, 1H), 6.41 (dd, 1H), 6.14 (m, 1H), 5.84 (dd, 1H), 4.17 (m, 4H), 3.97 (s, 3H), 1.88 (m, 2H), 1.68 (m, 2H), 1.40−1.25 (m, 14H). IR (ν): 3156 (w), 3120 (w), 2930 (s), 2858 (w), 1718 (m), 1637 (w), 1620 (w), 1573 (w), 1468 (w), 1410 (w), 1349 (s), 1332 (s), 1297 (m), 1225 (m), 1179 (s), 1134 (s), 1053 (s), 985 (w), 846 (w), 812 (w), 789 (w), 762 (w), 740 (m), 653 (m). M.p.: 7 °C.

Poly(1-(2-acryloyloxyundecyl)-3-methylimidazolium Bromide) (PM2Br). M2-Br was polymerized through conventional free radical polymerization. M2-Br (5.01 g, 12.9 mmol) and AIBN (0.02 g, 0.13 mmol) were dissolved in 20 mL of methanol and purged with nitrogen for 1 h. After reacting at 65 °C for 22 h, the reaction was terminated by immersing the flask in liquid nitrogen and freezing the mixture. The polymer was dialyzed against water for 8 days and then freeze-dried (4.12 g yield). The long dialysis time was to ensure product purity. The obtained product was a pale, yellowish solid. The NMR spectrum of the product is given in Figure S6A, and the IR spectrum is in Figure S7. ^{1}HNMR (500 MHz, MeOD, δ, ppm): 9.23−9.08 (s, 1H), 7.80−7.60 (m, 2H), 4.42−4.21 (s, 2H), 4.13−3.92 (m, 5H), 2.59−2.18 (m, 1H), 2.09−1.88 (s, 2H), 1.77−1.59 (s, 2H), 1.51−1.19 (m, 13H). IR (ν): 3676 (w), 3412 (w), 3148 (w), 3078 (w), 2988 (m), 2972 (w), 2920 (s), 2901 (s), 2853 (s), 1730 (m), 1572 (m), 1466 (w), 1452 (w), 1394 (m), 1381 (w), 1250 (m), 1233 (w), 1163 (s), 1076 (s), 1067 (s), 1057 (s), 868 (w), 752 (w), 721 (w), 650 (w), 619 (m). T_g: 0.6 °C.

Poly(1-(2-acryloyloxyundecyl)-3-methylimidazolium Bis-(trifluoromethane)sulfonimide) (Poly(M2)). PM2Br was anion-exchanged in order to obtain poly(M2). PM2Br (1.05 g, 2.7 mmol) was dissolved in 200 mL water. Aqueous LiNTf2 (0.82 g, 2.8 mmol in 20 mL water) was added into the PM2Br solution under vigorous stirring. The precipitated polymer was washed several times with water and then dried under vacuum (2 h, < 2 mbar) (0.59 g yield). NMR spectrum of the product is available in Figure S6B and IR spectrum in Figure S7. ^{1}HNMR (500 MHz, acetone-d6, δ, ppm): 9.08−8.96 (s, 1H), 7.83−7.64 (m, 2H), 4.47−4.27 (s, 2H), 4.19−3.89 (s, 3H), 2.91−2.73 (s, 2H), 2.52−2.15 (s, 1H), 2.04−1.86 (s, 2H), 1.85−1.58 (s, 2H), 1.59−1.10 (m, 12H). IR (ν): 3665 (w), 3155 (w),

3119 (w), 2928 (m), 2827 (m), 1730 (m), 1574 (w), 1468 (w), 1348 (s), 1331 (s), 1229 (m), 1179 (s), 1134 (s), 1053 (s), 847 (w), 789 (m), 762 (w), 739 (m), 652 (m), 613 (s), 600 (s). T_g: −37 °C.

Poly(1-vinyl-3-ethyl imidazolium Bromide) (PVEImBr). VEImBr (20.06 g, 99 mmol) and AIBN (0.16 g, 0.99 mmol) were dissolved in 40 mL of methanol. The mixture was purged with nitrogen for 1 h and then reacted at 60 °C for 23 h. The reaction was terminated by freezing the mixture with liquid nitrogen. The polymer was purified by dialysing against water for 4 days and then isolated by freeze-drying (16.00 g yield). The NMR spectrum is available in Figure S8. ^{1}HNMR (500 MHz, MeOD, δ, ppm): 8.30−7.50 (m, 3H), 4.86−4.48 (m, 1H), 4.47−4.12 (m, 2H), 3.31−2.19 (2H), 1.77−1.30 (3H). IR (ν): 3402 (m), 3127 (w), 3057 (m), 2986 (m), 2882 (w), 1634 (w), 1568 (m), 1549 (s), 1447 (m), 1435 (m), 1385 (w), 1339 (w), 1310 (w), 1269 (w), 1198 (w), 1159 (s), 1126 (m), 1059 (w), 1032 (w), 961 (w), 831 (m), 752 (m). T_g: 219 °C.

PEDOT-PIL. A filler material to be used in the preparation of conductive composites was prepared according to Marcilla et al.[38] EDOT (7.02 g, 49.4 mmol) and PVEImBr (10.26 g, 50.5 mmol repeating units) were dissolved in 250 mL water. APS (11.25 g, 49.3 mmol), dissolved in 250 mL water, was added slowly into vigorously stirred PVEImBr-EDOT dispersion. The mixture was stirred at room temperature for 3 days. A dark blue, almost black dispersion formed as a result. A portion of the dispersion was taken aside and stirred vigorously. Aqueous LiNTf2 (1.1 equiv of the repeating units of PVEImBr) was added dropwise into the dispersion. PEDOT−PIL precipitated and was recovered by filtration. The product was washed several times with water and dried under vacuum at 50 °C (4 h, < 2 mbar). The product was a dark blue powder. IR (ν): 3141 (w), 3098 (w), 2992 (w), 2929 (w), 1571 (w), 1548 (w), 1520 (w), 1497 (w), 1473 (w), 1452 (w), 1414 (w), 1393 (w), 1342 (s), 1324 (s), 1181 (s), 1128 (s), 1049 (s), 981 (m), 937 (w), 923 (w), 901 (w), 840 (m), 790 (m), 763 (w), 740 (m), 693 (w).

2.3. General Procedure for the Preparation of Films (Exemplified with a Film with 70:30 M1:M2 and 5 wt % OMMT). OMMT (0.30 g), CL (0.22 g, 0.25 mmol), M2 (2.14 g, 3.6 mmol), and M1 (3.52 g, 8.7 mmol) were ground in a mortar, and then sonicated with a Hielscher UP400S ultrasonic processor for 30 min. After mixing in the photoinitiator TMDPO (0.09 g, 0.25 mmol), the mixture was spread on a mold and polymerized using a setup of four 9 W UV lamps at wavelength of 365 nm for 1.5 h. The polymerized composite was washed with methanol and then dried. The absence of unreacted monomer was verified by means of FTIR spectroscopy. In particular, the absence of bands around 1650 and 950 cm^{-1} that arise from alkene groups was checked. The IR spectrum of the composite with 70:30 ratio of M1 and M2 and with 5 wt % OMMT is given in Figure S9 alongside the spectra of the monomers M1 and M2, as well as the filler (OMMT). The PEDOT−PIL-filled composites were prepared in the same manner with the exception that PEDOT−PIL was used in place of OMMT.

When preparing composites with different M1−M2 ratios, the relative amounts of the IL monomers were adjusted, but the synthesis was performed otherwise as described above. In each composite film the amount of cross-linker was 2 mol %. The amount of initiator was always 2% of the IL monomers. The amount of OMMT was measured with respect to the total mass of the rest of the mixture.
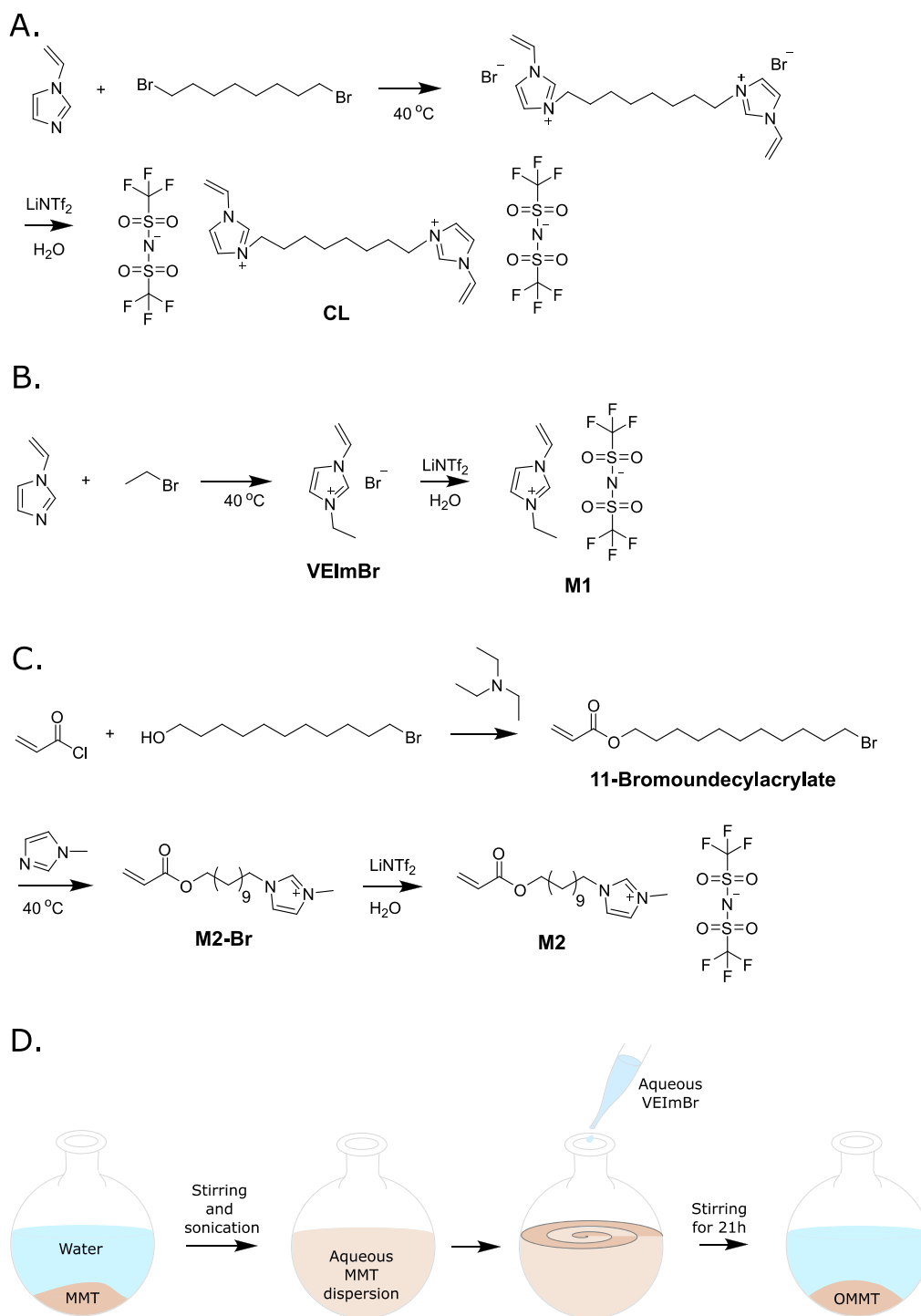
2.4. Instrumentation. *Nuclear Magnetic Resonance (NMR).* NMR spectra were recorded using a Bruker Avance III 500 spectrometer.

Fourier Transform Infrared Spectroscopy (FTIR). Infrared spectroscopy was conducted on Shimadzu IRTracer-100 Fourier transform infrared spectrophotometer at room temperature in the wavenumber range of 600−4000 cm^{-1}.

Stress−Strain Measurements. The films were stretched at 25 °C, 10 μm/s until breakage using a TA Instruments DMA Q800. The measurement was repeated at least three times, and the results were averaged.

Thermogravimetric Measurements (TGA). The samples were heated 25−800 °C 10 °C/min under nitrogen atmosphere using Netzsch STA 449 F3 instrument.

Scheme 1. Schematic Illustrations of the Syntheses of A. CL, B. M1, C. M2, and D. Organoclay (OMMT)

A.

B.

VEImBr

M1

C.

11-Bromoundecylacrylate

M2-Br

M2

D.

Water → MMT

Stirring and sonication →

Aqueous MMT dispersion

Aqueous VEImBr →

Stirring for 21h →

OMMT

Oscillatory Modulus Measurements. The films' storage and loss moduli were measured as a function of temperature. The measurements were conducted with a TA Instruments DMA Q800 instrument. The moduli were measured from −50 to 250 °C, 10 °C/min. The strain amplitude was 0.1% with a frequency of 1 Hz.

Differential Scanning Calorimetry (DSC). DSC measurements were carried out on a TA Instruments DSC Q2000 calorimeter, heating the samples up to 250 °C, 10 °C/min. The starting temperature was −90 °C for PEDOT−PIL composites and −60 °C for the clay composites.

*Scanning Electron Microscopy (SEM).* Tensile fracture surfaces were imaged using Hitachi S-4800 FESEM with an acceleration voltage of 3 kV. The samples were coated with a thin layer of Au−Pd prior to measurements.

Four Point Probe. Using rectangular samples, sheet resistances of the composites were measured at room temperature by a four-point probe technique using Jandel RM3000+ test unit.

3. RESULTS AND DISCUSSION

This article reports a facile preparation method of flexible PIL composites by photopolymerization of a mixture of two ionic liquid monomers (IL monomers). Our previous contribution presented series of clay-filled composites with a matrix consisting of a polymerized vinylimidazolium-based ionic

Scheme 2. Schematic Illustration of the Composite Preparation Method
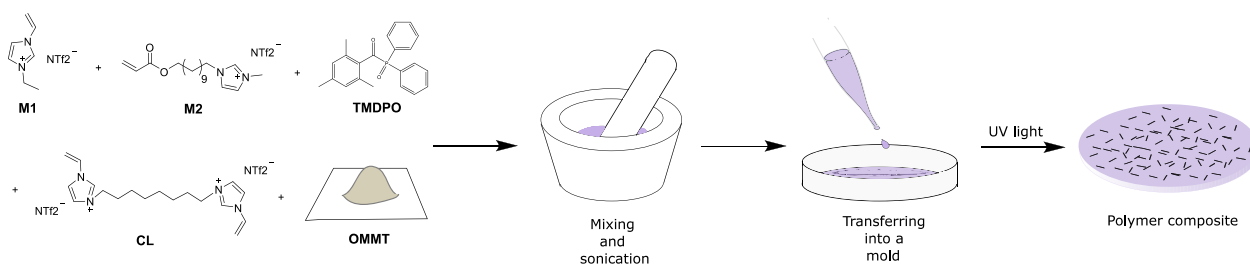
liquid, M1.[11] The materials were glassy and somewhat inflexible at room temperature. This article explores the possibilities of fabricating softer materials by copolymerization while retaining the IL-like solvent qualities of the monomers.

Mechanical properties of a material relate to the glass transition temperature (T_g), i.e., polymers with a high glass transition temperature tend to be brittle.[34] In our previous work, polymerized M1 exhibited a T_g of approximately 67 °C, and the material was brittle.[11] Therefore, it was hypothesized that lowering the T_g would make the materials more durable. To achieve this, M1 was copolymerized with another ionic liquid monomer, M2. The methacrylate derivative of polymerized M2 exhibits a T_g value of −29 °C, and since acrylate polymers exhibit lower T_gs than corresponding methacrylates, polymeric M2 was expected to have a T_g low enough to soften the composites already at low contents.[39,40] Indeed, homopolymer of M2, poly(M2), exhibited a T_g value of −37 °C (see Figure S10 for the DSC trace). For comparison, the T_g of PM2Br, the bromide bearing equivalent of poly(M2), was 0.6 °C. This attests to the NTf$_2$-anion's tendency to give polymers with relatively low T_g values.[3] It should be noted that the molar masses of polymers were not determined since polyelectrolytes have a strong tendency to interact with size exclusion chromatography column materials.[41] The composites were cross-linked with CL in order to further improve their durability. The syntheses of the used monomers and organoclay are given in Scheme 1

M1 was synthesized through anion metathesis from its bromide bearing equivalent, VEImBr. The anion exchange showed that the chemical shifts of the imidazolium ring protons—especially the N−CH−N proton—was higher for M1 than for VEImBr (Figure S1). However, it should be noted that the measurements were made in different solvents. The chemical shift of the N−CH−N proton was located at 8.98 ppm for VEImBr when measured in deuterated water, while the shift was observed at 9.37 ppm for M1 that was measured in deuterated acetone. This arises from the fact that the chemical shifts of the imidazolium ring protons are sensitive to their surroundings, e.g. cation−anion interactions.[42,43] The inclusion of NTf$_2$ anions was also checked by means of FTIR spectroscopy. In particular, a strong band around 1340 cm^{-1}, which arises from the anion, is seen in the ion-exchanged product (Figure S2A).

Likewise, M2 was prepared through an anion exchange. The inclusion of NTf$_2$-anions resulted in a major downshift in the imidazolium ring proton chemical shifts (see Figure S5). The N−CH−N proton shift shifted from 10.58 to 8.78 ppm when the bromide counterion was switched to NTf$_2$. Similar observations have been made for a similar monomer with tetrafluoroborate as the counterion.[37]

The next section discusses the effects of the IL monomer ratio on material properties. The monomer ratio which gave the toughest materials was then utilized in clay composites of different filler loadings.

3.1. Clay-Filled Polymer Composites: The Effect of IL Monomer Ratio. M1−M2 copolymer composites were prepared with several M1−M2 ratios. The monomer ratio was varied so that the IL monomer content varied from 100% M1 to 100% M2. Stated another way, M1 was gradually replaced with M2, until eventually M2 was the only IL monomer used in the mixture. Each composite was cross-linked with 2% chemical cross-linker. In order to assess the different mixtures' ability to disperse clay, each composite was filled with 5 wt % organoclay (OMMT). The composite preparation methodology is illustrated in Scheme 2.

The composites were softer and more pliable the more M2 they contained. Each composite appeared even with no visible clay aggregates (see Figure S11 for examples). For comparison, a series of films were prepared from a mixture of butyl acrylate and M1. Inclusion of butyl acrylate successfully lowered the T_g (Figure S12). However, copolymerization with a nonionic monomer resulted in severe phase separation, as can be seen in the photographs in Figure S13 in SI. This attests to the IL monomers' superior ability to disperse clay.

The M1−M2 composites' glass transition temperatures were measured by means of DMA and DSC. The results are presented in Figure 1. As expected, the T_g decreases with
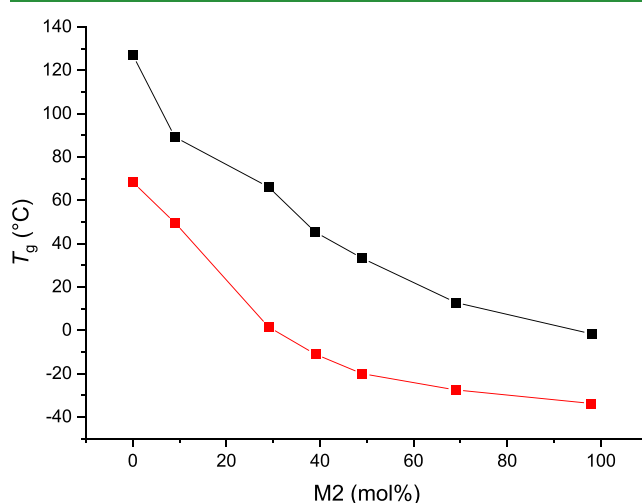

Figure 1. Glass transition temperatures of M1−M2 composites as a function of M2-content of the feed measured with DMA (black) and DSC (red). The composites are filled with 5 wt % organoclay and cross-linked with 2 mol % cross-linker. The DMA T_g was defined as the peak of tan δ curve. The definition of T_g using tan δ is illustrated in Figure S20.
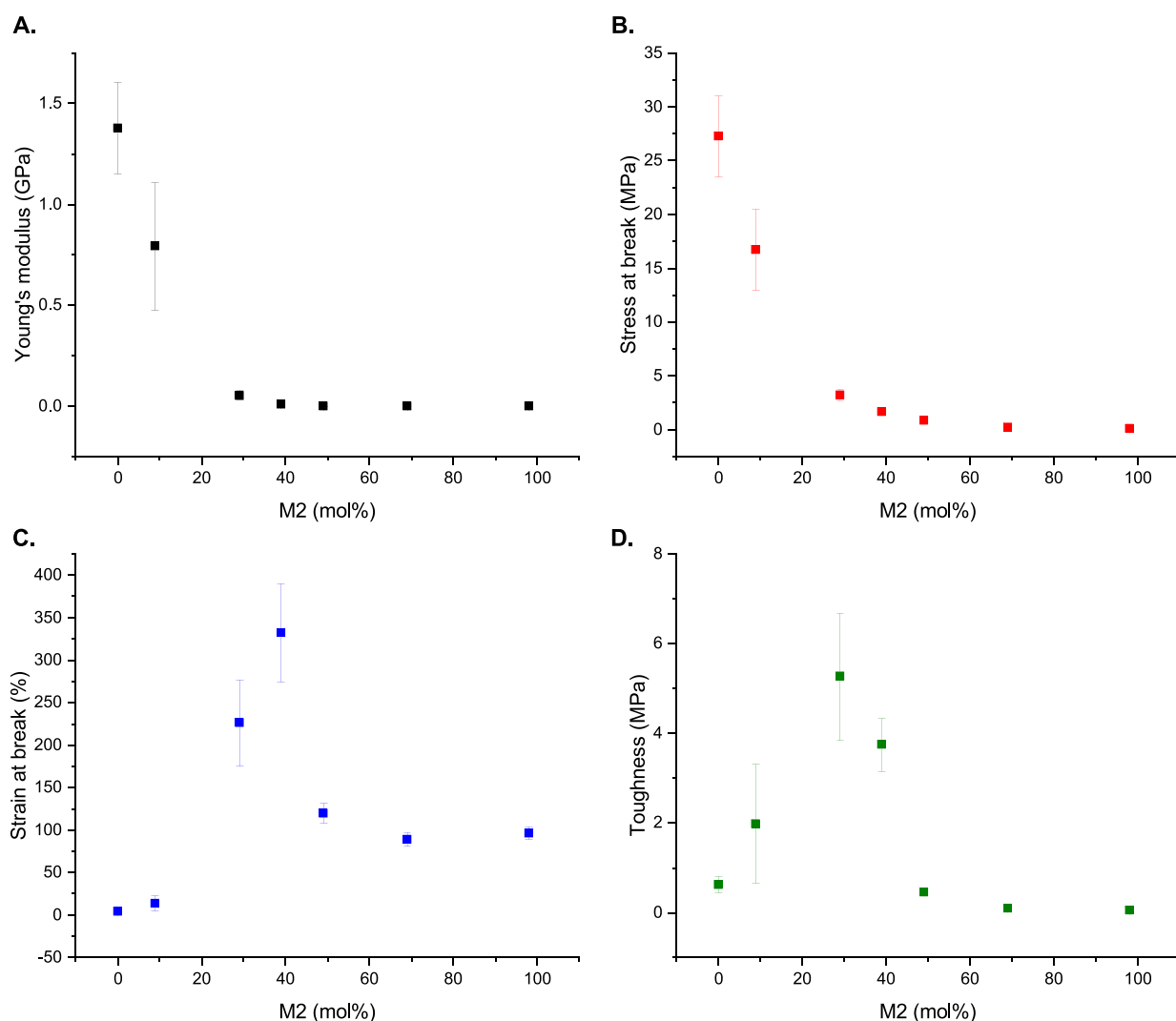
Figure 2. Tensile properties of M1−M2 composites as a function of the M2 content, i.e., the molar percentage of M2 in the feed. Each composite has been filled with 5 wt % organoclay and cross-linked with 2% chemical cross-linker. A. Young's modulus (black), B. Stress at break (red), C. Strain at break (blue), and D. Toughness of the composites (green). Toughness was defined as the area below the stress−strain curve. The results are averages of three measurements. For some samples, the error bars are the same size or smaller than the symbols and thus not visible.

increasing M2 content. The T_gs can be readily adjusted from subzero temperatures to over 100 °C by altering the ratio of M1 and M2 in the feed.

The mechanical properties of M1−M2 copolymer films were characterized by stress−strain measurements. The results are presented in Figure 2. The Young's modulus and stress at break decrease with increasing fraction of M2 in the feed, while the strain at break increases with added M2. The strain at break peaks with approximately 40 mol % M2 in the feed (Figure 2C). The maximum value is approximately 80 times that of the M1-homopolymer. Figure 2D shows the toughness as a function of M2 content. Toughness was defined as the area under the stress−strain curve. According to Figure 2D, the M1−M2-composites are the toughest when there is approximately 30 mol % M2 in the feed. The toughness of said composite exhibited an 8-fold increase compared to the M1-homopolymer. This indicates that a copolymer matrix provides superior materials as opposed to a homopolymer matrix.

Copolymer matrix exhibited lower resistance to thermal degradation than either homopolymer, as depicted in Figure S14 in SI. This might be related to the higher heterogeneity of

the copolymer, as opposed to the corresponding homopolymers. However, the reason remains unclear.

3.2. Clay-Filled Copolymer Composites: The Effect of Filler Loading. The M1−M2 ratio which gave the toughest composite (70:30 M1:M2) was used in the preparation of a series of clay composites. The composites were filled with organoclay, OMMT, and filler loading was varied from 0 to 50 wt %. That is, unlike in the previous section, this series also includes a nonfilled film. The M1:M2 ratio was 70:30 in each composite.

The effect of clay content on the composites' fracture surface morphology was studied with scanning electron microscopy (SEM). SEM images of the composites are collected in Figure 3. For comparison, a SEM image of the filler itself is given in Figure 4. The fracture surface of plain film appears relatively even, only exhibiting wave-like ridges arising from plastic deformation of the material (Figure 3A). Figure 3B−D suggest that when filler is added, the portion of clay-free, smooth regions decreases. Eventually, with the highest filler loading, the fracture surface is highly uneven and entirely covered with clay aggregates.
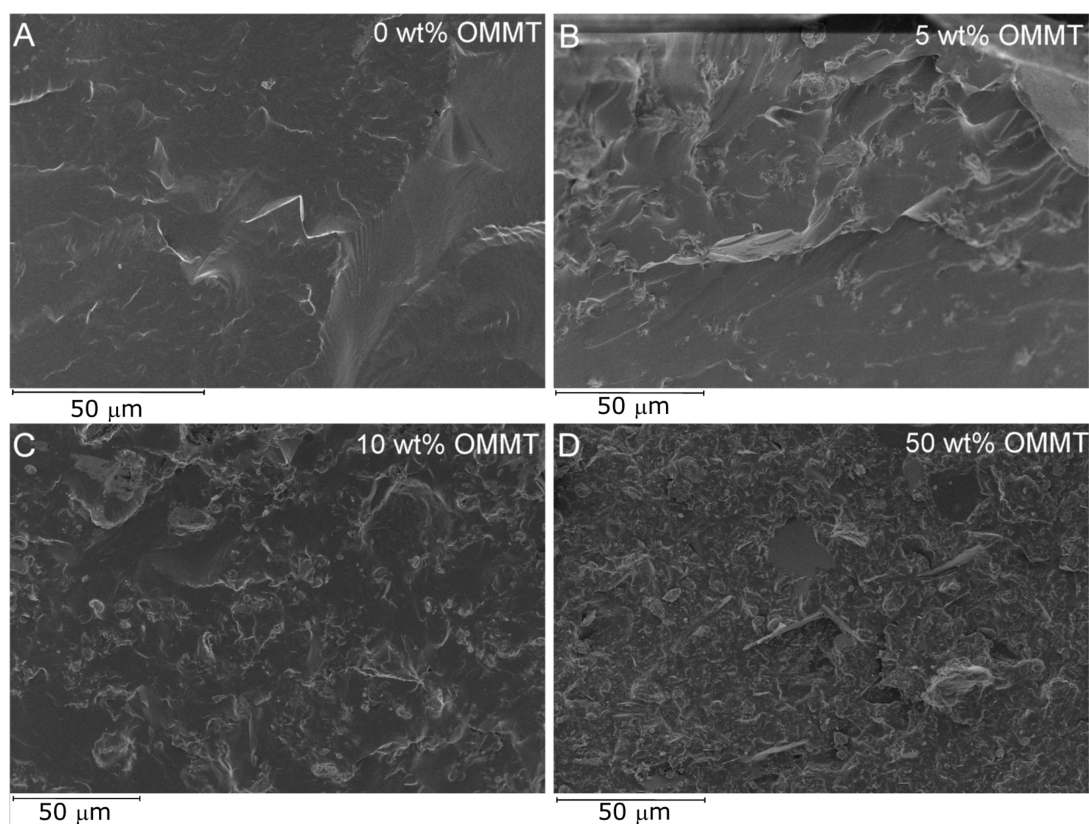
Figure 3. Representative cross-section SEM images of 70:30 M1:M2 composites prepared with A. 0 wt %, B. 5 wt %, C. 10 wt %, and D. 50 wt % OMMT in the feed.
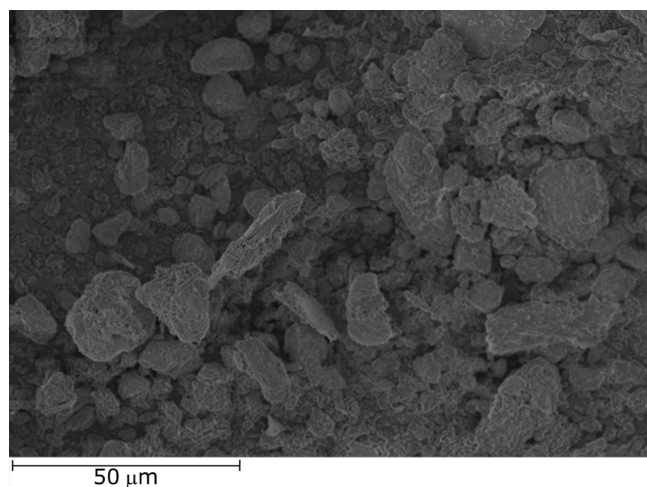

Figure 4. SEM image of the filler (OMMT).

With the highest filler loading (Figure 3D), the fracture surface exhibits apparent clay stacks that the ionic liquids were not able to separate. The amount of clay was so high that the ionic liquids were not able to wet the clay entirely, thus resulting in incomplete filler dispersion. The presence of clay aggregates was verified by means of EDX elemental mapping (see Figure S15).

Tensile tests were performed to assess the mechanical properties of the composites. Figure 5 shows the tensile properties of the films in dependence of filler loading. Clay provided improvements in stiffness and strength, but decreased the material's ductility and hence its toughness.

Both the stiffness and strength increase rather steadily with increasing filler loading, and 5-fold and 1.5-fold enhancements were observed for Young's modulus and stress at break, respectively. The increase in rigidity was ascribed to the filler particles restricting the mobility of the matrix. Improved strength suggests that the filler is able to support stress transfer between the filler and the matrix.[44] It is worth noting that the stiffness and strength increased all the way up to the highest filler loading, 50 wt %. For comparison, in our earlier work on glassy composites the material properties started to deteriorate after exceeding filler loadings of approximately 5 wt %.[11] This shows that the copolymer matrix is able to take up significantly higher filler loadings without adverse effects on the material strength. It was suspected that either M2 had an excellent ability to interact with the filler, or the softness of the copolymer matrix allowed more even matrix/filler contact, as opposed to the stiffer poly(M1) chains in our previous work.

Meanwhile, ductility of the most highly filled composite was only approximately 20% and toughness 30% of that of the unfilled matrix. Particulate additives have a tendency to embrittle ductile materials.[45,46] The filler particles obstruct the movements of the polymer chains, which increases the material's brittleness.[47]

The filler's effect on thermal stability was studied by means of thermogravimetry. Figure 6 depicts the degradation temperatures and char yields in dependence of filler loading. The degradation temperatures were determined in three ways: 1) the temperature at which 2 wt % of the material degraded, starting from 150 °C, 2) the inflection point, and 3) the intersection of two tangents, one drawn at the point of the steepest mass loss and the other tangent before the material
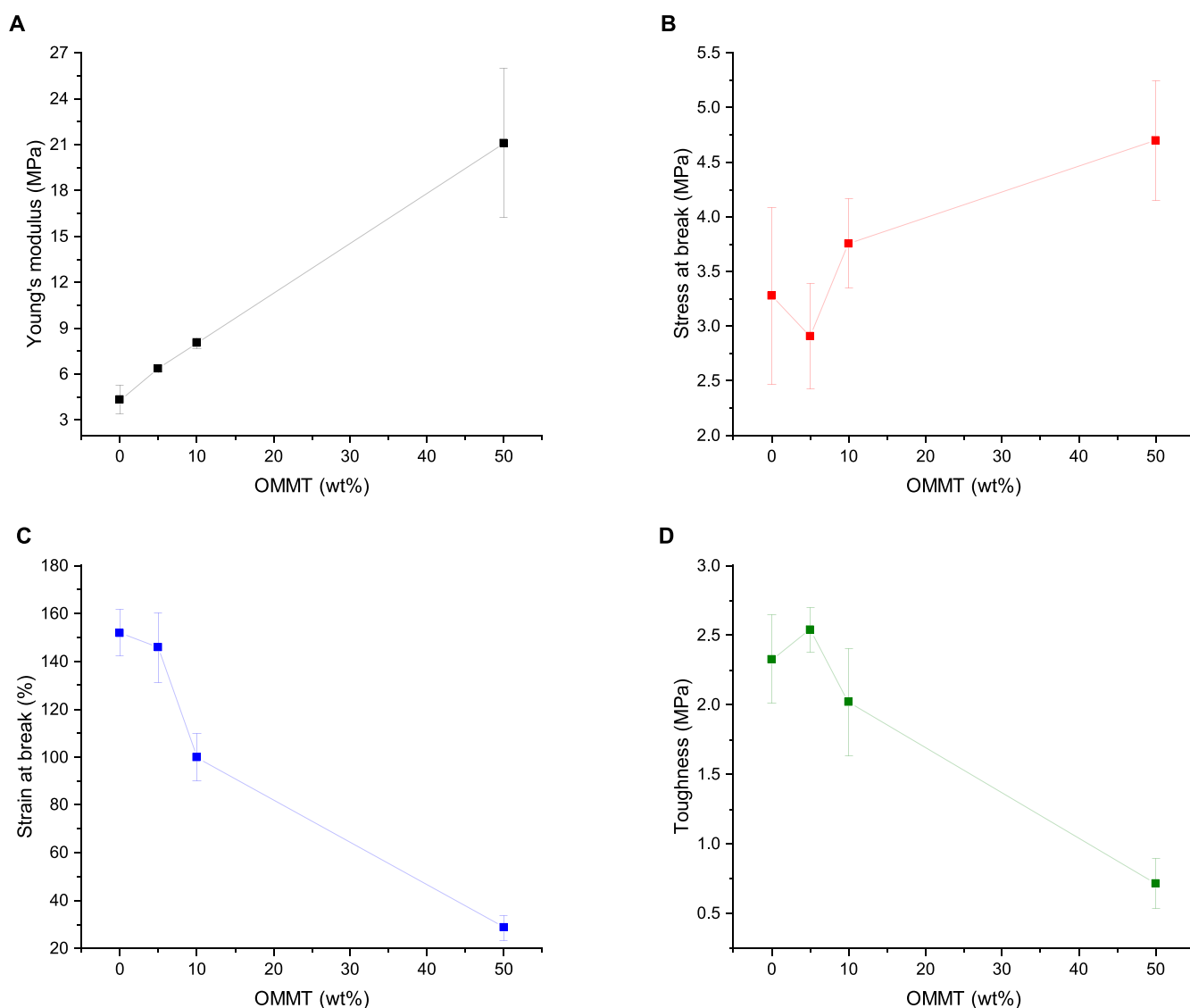
Figure 5. Tensile properties of flexible, clay-filled 70:30 M1:M2 composites. A. Young's modulus (black), B. Stress at break (red), C. Strain at break (blue), and D. Toughness of composites (green) in dependence of filler loading. Toughness was defined as the area below the stress−strain curve. The results are averages of three measurements.

starts to degrade. Illustrations of the definitions are given in Figure S16.

The composites' resistance to thermal degradation increases at first, being the highest with 10 wt % OMMT in the feed. From thereon, the thermal stability degrades. Particularly prominent enhancement in thermal stability is observed when the degradation onset is defined as the intersection of two tangents. The degradation temperature of the composite with 10 wt % clay is over 50 °C higher than the degradation temperature of the plain matrix. An enhancement of similar magnitude has been observed for polypropylene, for instance, although the filler loading was only 5 wt %.[48] The enhanced thermal stability of MMT composites was attributed to the clay platelets obstructing the diffusion of decomposition products.[48]

The deterioration of thermal stability at the highest filler loading was ascribed to filler aggregation. The clay platelets' ability to delay the thermal degradation is highly dependent on the quality of filler dispersion. If the clay is not dispersed evenly, the platelets do not hinder the volatiles as effectively, and the material degrades at relatively low temperatures.[49]

The char yield given by TGA (Figure 6B, black symbols) is a sum of the nonvolatile remnants of clay as well as remains of the matrix itself. The char yield of the unfilled material was 4.8 wt %, while the residual mass of the organoclay itself was 90.8 wt % (see Figure S17 for the TGA curve of OMMT). Using these values, the amounts of char that the composites should theoretically yield were calculated and plotted in Figure 6B as red symbols. The experimental and theoretical values are in agreement apart from the composite prepared with 50 wt % OMMT. Theoretically, the char yield should be approximately 50 wt % when 50 wt % OMMT is added into the mixture. However, the experimentally obtained char yield was only around 35 wt %. This suggests that the ionic liquid mixture was not able to bind all of the added clay when the clay content is high. However, with moderate clay contents, the values agree well. This indicates that the contents of the components are similar in the final product as they are in the feed below 50 wt % OMMT.
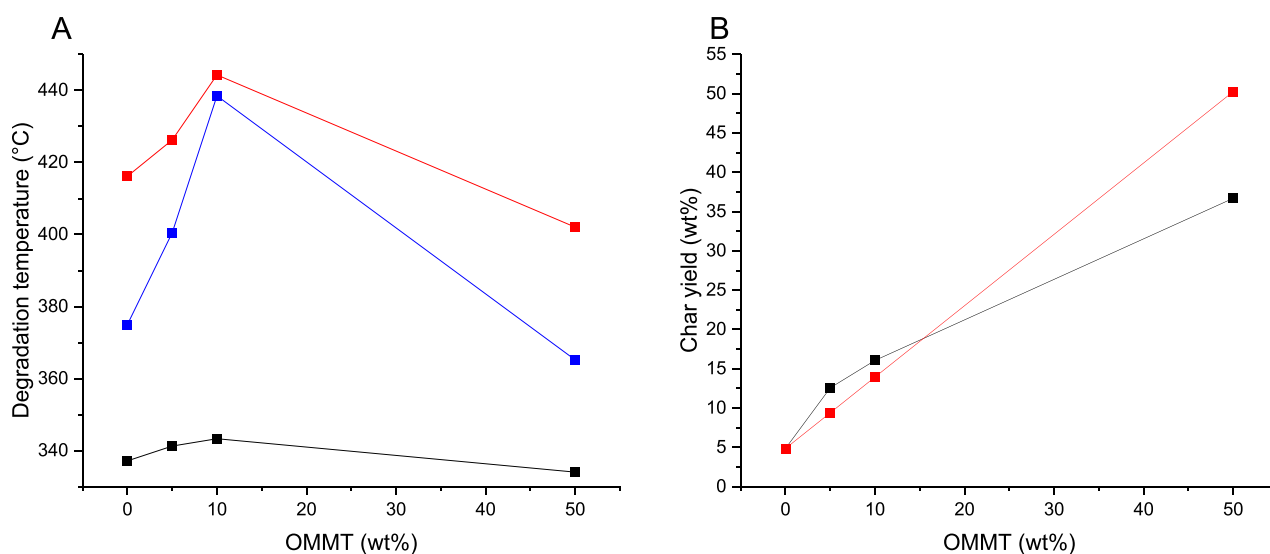
Figure 6. A. The degradation temperature of the 70:30 M1−M2 composites in dependence of OMMT-loading defined as the point where, from 150 °C onward, 2% of the material had degraded (black), the temperature at the steepest weight loss (red) and the intersection of two tangents (blue). B. Theoretical (red) and experimentally obtained (black) char yield in dependence of filler loading.

Dynamic mechanical analysis (DMA) and differential scanning calorimetry (DSC) were used to determine the glass transition temperatures (T_g) of the composites. The obtained values are illustrated in Figure 7, and the numerical values are given in Table S1 in SI. The tan δ, loss modulus, and storage modulus curves are given in Figure S18, and the DSC traces in are in Figure S19 in SI.
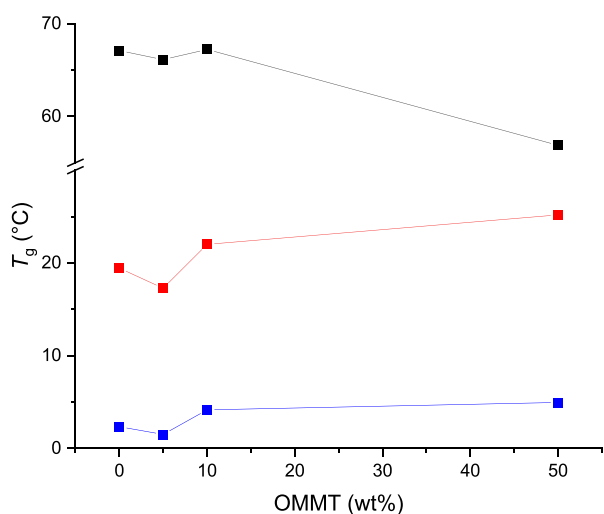

Figure 7. T_gs of the OMMT-filled 70:30 M1:M2 composites as a function of filler loading. DMA T_gs were defined as the peak of tan δ (black), and peak of loss modulus (E") (red). T_g values obtained by DSC are given as blue symbols.

The peak of tan δ stays constant until the highest filler loading, where the T_g value drops significantly. The drop in T_g was ascribed to the aggregation of excess filler. Similar behavior has been reported for poly(methyl methacrylate)/montmorillonite composites, for instance.[50]

It is also worth noting that the magnitude of tan δ peak decreases with added filler, as is often the case for filled materials.[51,52] The other T_gs, i.e. peak of loss modulus and DSC appear to give slightly higher T_g values with increasing

filler loading. The definitions of $T_g(\tan \delta)$ and $T_g(E")$ are illustrated in Figure S20.

In order to test the IL mixture's suitability for dispersing other materials, the optimized M1−M2 matrix (70:30 M1:M2) was also used in the preparation of composites in which the filler material was a conductive polymer. The results are presented in SI (see pages S12−S19), and it is seen that the usage of conductive filler particles increases the conductivity of the materials, while still yielding materials with appreciable mechanical properties.

4. CONCLUSIONS

Material properties of IL based composites were successfully adjusted by means of copolymerization. Polymer composites were prepared by using different combinations of two different ionic liquid monomers. It was found that by changing the relative amounts of the two used IL monomers, T_g values of the composites could be adjusted within a range of approximately 100 °C. Likewise, tensile strength and stiffness could be readily tuned by only changing the amounts of used monomers. The ductility and toughness were found to be the greatest when a copolymer matrix was used—toughness, for instance, was up to 8 times as high as the toughness of the respective homopolymers.

Copolymer composites were prepared using montmorillonite clay and conductive polymer particles as filler materials. The matrix material was able to take up large amounts of montmorillonite clay while still gaining improvements in mechanical properties. When conductive polymer particles were used as the filler material, the mechanical strength was impaired slightly, but the material became more conductive. In effect, the methodology yielded mechanically satisfactory and conductive all-polymer composites.

Using a combination of different ionic liquids to disperse fillers and constitute polymer composites is a versatile and straightforward approach for composite preparation. The option to use different monomers and fillers makes the presented methodology highly promising.

■ ASSOCIATED CONTENT

Ⓢ Supporting Information

The Supporting Information is available free of charge at https://pubs.acs.org/doi/10.1021/acsapm.3c00601.

Additional results, including 1HNMR and IR spectra, photographs, SEM images, elemental maps, DSC, TGA, and DMA results (PDF)

■ AUTHOR INFORMATION

Corresponding Authors

Erno Karjalainen − *VTT Technical Research Centre of Finland Ltd., FI-02044 VTT Espoo, Finland;* ⓞ orcid.org/0000-0001-9247-813X; Email: erno.karjalainen@alumni.helsinki.fi

Vladimir O. Aseyev − *Department of Chemistry, University of Helsinki, FIN-00014 HY Helsinki, Finland;* ⓞ orcid.org/0000-0002-3739-8089; Email: vladimir.aseyev@helsinki.fi

Authors

Linda Salminen − *Department of Chemistry, University of Helsinki, FIN-00014 HY Helsinki, Finland;* ⓞ orcid.org/0000-0002-0731-5254

Heikki Tenhu − *Department of Chemistry, University of Helsinki, FIN-00014 HY Helsinki, Finland;* ⓞ orcid.org/0000-0001-5957-4541

Complete contact information is available at:
https://pubs.acs.org/10.1021/acsapm.3c00601

Author Contributions

The manuscript was written through contributions of all authors. All authors have given approval to the final version of the manuscript.

Notes

The authors declare no competing financial interest.

■ ACKNOWLEDGMENTS

■ REFERENCES

(1) Zhang, M.; Semiat, R.; He, X. Recent Advances in Poly(Ionic Liquids) Membranes for CO2 Separation. *Sep. Purif. Technol.* **2022**, *299*, 121784.

(2) Zhang, S. Y.; Zhuang, Q.; Zhang, M.; Wang, H.; Gao, Z.; Sun, J. K.; Yuan, J. Poly(Ionic Liquid) Composites. *Chem. Soc. Rev.* **2020**, *49* (6), 1726−1755.

(3) Green, M. D.; Salas-De La Cruz, D.; Ye, Y.; Layman, J. M.; Elabd, Y. A.; Winey, K. I.; Long, T. E. Alkyl-Substituted N-Vinylimidazolium Polymerized Ionic Liquids: Thermal Properties and Ionic Conductivities. *Macromol. Chem. Phys.* **2011**, *212* (23), 2522−2528.

(4) Marcilla, R.; Blazquez, J. A.; Rodriguez, J.; Pomposo, J. A.; Mecerreyes, D. Tuning the Solubility of Polymerized Ionic Liquids by Simple Anion-Exchange Reactions. *J. Polym. Sci. Part A Polym. Chem.* **2004**, *42* (1), 208−212.

(5) Marcilla, R.; Blazquez, J. A.; Fernandez, R.; Grande, H.; Pomposo, J. A.; Mecerreyes, D. Synthesis of Novel Polycations Using the Chemistry of Ionic Liquids. *Macromol. Chem. Phys.* **2005**, *206* (2), 299−304.

(6) Vygodskii, Y. S.; Mel'nik, O. A.; Shaplov, A. S.; Lozinskaya, E. I.; Malyshkina, I. A.; Gavrilova, N. D. Synthesis and Ionic Conductivity of Polymer Ionic Liquids. *Polym. Sci. - Ser. A* **2007**, *49* (3), 256−261.

(7) Cui, J.; Nie, F. M.; Yang, J. X.; Pan, L.; Ma, Z.; Li, Y. S. Novel Imidazolium-Based Poly(Ionic Liquid)s with Different Counterions for Self-Healing. *J. Mater. Chem. A* **2017**, *5* (48), 25220−25229.

(8) Liu, Y.; Zhao, J.; He, F.; Zheng, C.; Lei, Q.; Zhao, X.; Yin, J. Ion Transport, Polarization and Electro-Responsive Elelctrorheological Effect of Self-Crosslinked Poly(Ionic Liquid)s with Different Counterions. *Polymer (Guildf).* **2019**, *177*, 149−159.

(9) Karjalainen, E.; Chenna, N.; Laurinmäki, P.; Butcher, S. J.; Tenhu, H. Diblock Copolymers Consisting of a Polymerized Ionic Liquid and Poly(N-Isopropylacrylamide). Effects of PNIPAM Block Length and Counter Ion on Self-Assembling and Thermal Properties. *Polym. Chem.* **2013**, *4* (4), 1014−1024.

(10) Karjalainen, E.; Aseyev, V.; Tenhu, H. Counterion-Induced UCST for Polycations. *Macromolecules* **2014**, *47*, 7581−7587.

(11) Salminen, L.; Karjalainen, E.; Aseyev, V.; Tenhu, H. Well-Dispersed Clay in Photopolymerized Poly(Ionic Liquid) Matrix. *Mater. Chem. Phys.* **2022**, *292*, 126805.

(12) Bonhôte, P.; Dias, A. P.; Papageorgiou, N.; Kalyanasundaram, K.; Grätzel, M. Hydrophobic, Highly Conductive Ambient-Temperature Molten Salts. *Inorg. Chem.* **1996**, *35* (5), 1168−1178.

(13) Maksym, P.; Tarnacka, M.; Dzienia, A.; Erfurt, K.; Chrobok, A.; Zięba, A.; Wolnica, K.; Kaminski, K.; Paluch, M. A Facile Route to Well-Defined Imidazolium-Based Poly(Ionic Liquid)s of Enhanced Conductivity via RAFT. *Polym. Chem.* **2017**, *8*, 5433.

(14) Tang, J.; Sun, W.; Tang, H.; Radosz, M.; Shen, Y. Enhanced CO2 Absorption of Poly(Ionic Liquid)S. *Macromolecules* **2005**, *38* (6), 2037−2039.

(15) Pera-Titus, M. Porous Inorganic Membranes for CO2 Capture: Present and Prospects. *Chem. Rev.* **2014**, *114* (2), 1413−1492.

(16) Bara, J. E.; Lessmann, S.; Gabriel, C. J.; Hatakeyama, E. S.; Noble, R. D.; Gin, D. L. Synthesis and Performance of Polymerizable Room-Temperature Ionic Liquids as Gas Separation Membranes. *Ind. Eng. Chem. Res.* **2007**, *46* (16), 5397−5404.

(17) Tomé, L. C.; Isik, M.; Freire, C. S. R.; Mecerreyes, D.; Marrucho, I. M. Novel Pyrrolidinium-Based Polymeric Ionic Liquids with Cyano Counter-Anions: High Performance Membrane Materials for Post-Combustion CO2 Separation. *J. Membr. Sci.* **2015**, *483*, 155−165.

(18) Zhang, C.; Zhang, W.; Gao, H.; Bai, Y.; Sun, Y.; Chen, Y. Synthesis and Gas Transport Properties of Poly(Ionic Liquid) Based Semi-Interpenetrating Polymer Network Membranes for CO2/N2 Separation. *J. Membr. Sci.* **2017**, *528*, 72−81.

(19) Zarca, G.; Horne, W. J.; Ortiz, I.; Urtiaga, A.; Bara, J. E. Synthesis and Gas Separation Properties of Poly(Ionic Liquid)-Ionic Liquid Composite Membranes Containing a Copper Salt. *J. Membr. Sci.* **2016**, *515*, 109−114.

(20) Hu, X.; Tang, J.; Blasig, A.; Shen, Y.; Radosz, M. CO2 Permeability, Diffusivity and Solubility in Polyethylene Glycol-Grafted Polyionic Membranes and Their CO2 Selectivity Relative to Methane and Nitrogen. *J. Membr. Sci.* **2006**, *281* (1−2), 130−138.

(21) Kammakakam, I.; Bara, J. E.; Jackson, E. M.; Lertxundi, J.; Mecerreyes, D.; Tome, L. C. Tailored CO2-Philic Anionic Poly(Ionic Liquid) Composite Membranes: Synthesis, Characterization, and Gas Transport Properties. *ACS Sustain. Chem. Eng.* **2020**, *8*, 5954−5965.

(22) Grygiel, K.; Wicklein, B.; Zhao, Q.; Eder, M.; Pettersson, T.; Bergström, L.; Antonietti, M.; Yuan, J. Omnidispersible Poly(Ionic Liquid)-Functionalized Cellulose Nanofibrils: Surface Grafting and Polymer Membrane Reinforcement. *Chem. Commun.* **2014**, *50*, 12486.

(23) Vilela, C.; Sousa, N.; Pinto, R. J. B.; Silvestre, A. J. D.; Figueiredo, F. M. L.; Freire, C. S. R. Exploiting Poly(Ionic Liquids) and Nanocellulose for the Development of Bio-Based Anion-Exchange Membranes. *Biomass and Bioenergy* **2017**, *100*, 116−125.

(24) Fukushima, T.; Kosaka, A.; Yamamoto, Y.; Aimiya, T.; Notazawa, S.; Takigawa, T.; Inabe, T.; Aida, T. Dramatic Effect of Dispersed Carbon Nanotubes on the Mechanical and Electro-

conductive Properties of Polymers Derived from Ionic Liquids. *Small* **2006**, *2* (4), 554−560.

(25) Wang, X.; Zhu, H.; Girard, G. M. A.; Yunis, R.; Macfarlane, D. R.; Mecerreyes, D.; Bhattacharyya, A. J.; Howlett, P. C.; Forsyth, M. Preparation and Characterization of Gel Polymer Electrolytes Using Poly(Ionic Liquids) and High Lithium Salt Concentration Ionic Liquids. *J. Mater. Chem. A* **2017**, *5* (45), 23844−23852.

(26) Fdz De Anastro, A.; Lago, N.; Berlanga, C.; Galcerán, M.; Hilder, M.; Forsyth, M.; Mecerreyes, D. Poly(Ionic Liquid) Iongel Membranes for All Solid-State Rechargeable Sodium Battery. *J. Membr. Sci.* **2019**, *582*, 435−441.

(27) Xu, H.; Tong, F.; Yu, J.; Wen, L.; Zhang, J.; He, J. A One-Pot Method to Prepare Transparent Poly(Methyl Methacrylate)/Montmorillonite Nanocomposites Using Imidazolium-Based Ionic Liquids. *Polym. Int.* **2012**, *61* (9), 1382−1388.

(28) Liu, P. Polymer Modified Clay Minerals: A Review. *Appl. Clay Sci.* **2007**, *38* (1−2), 64−76.

(29) Ummartyotin, S.; Bunnak, N.; Manuspiya, H. A Comprehensive Review on Modified Clay Based Composite for Energy Based Materials. *Renew. Sustain. Energy Rev.* **2016**, *61*, 466−472.

(30) Galehassadi, M.; Hosseinzadeh, F.; Mahkam, M. Modification of Clays with Styrenic Ionic Liquid by Synthesis of In-Situ Polystyrene Nanocomposite. *e-Polym.* **2013**, *031*. DOI: 10.1515/epoly-2013-0131.

(31) Su, S.; Jiang, D. D.; Wilkie, C. A. Novel Polymerically-Modified Clays Permit the Preparation of Intercalated and Exfoliated Nanocomposites of Styrene and Its Copolymers by Melt Blending. *Polym. Degrad. Stab.* **2004**, *83* (2), 333−346.

(32) Jahed, F. S.; Galehassadi, M.; Davaran, S. A Novel 1,2,3-Benzotriazolium Based Ionic Liquid Monomer for Preparation of MMT/Poly Ionic Liquid (PIL) PH-Sensitive Positive Charge Nanocomposites. *J. Chem. Sci.* **2019**, *131* (18), 1−9.

(33) Puthumana, M.; Santhana Gopala Krishnan, P.; Nayak, S. K. Chemical Modifications of PLA through Copolymerization. *Int. J. Polym. Anal. Charact.* **2020**, *25* (8), 634−648.

(34) Negi, A.; Basu, S. A Molecular Dynamics Study on the Strength and Ductility of High Tg Polymers. *Model. Simul. Mater. Sci. Eng.* **2006**, *14*, 563−580.

(35) Brennecke, J. F.; Maginn, E. J. Ionic Liquids: Innovative Fluids for Chemical Processing. *AIChE J.* **2001**, *47* (11), 2384−2389.

(36) Cheng, S.; Zhang, M.; Wu, T.; Hemp, S. T.; Mather, B. D.; Moore, R. B.; Long, T. E. Ionic Aggregation in Random Copolymers Containing Phosphonium Ionic Liquid Monomers. *J. Polym. Sci. Part A Polym. Chem.* **2012**, *50* (1), 166−173.

(37) Yan, F.; Texter, J. Solvent-Reversible Poration in Ionic Liquid Copolymers. *Angew. Chemie - Int. Ed.* **2007**, *46* (14), 2440−2443.

(38) Marcilla, R.; Ochoteco, E.; Pozo-Gonzalo, C.; Grande, H.; Pomposo, J. A.; Mecerreyes, D. New Organic Dispersions of Conducting Polymers Using Polymeric Ionic Liquids as Stabilizers. *Macromol. Rapid Commun.* **2005**, *26* (14), 1122−1126.

(39) Shaplov, A. S.; Lozinskaya, E. I.; Ponkratov, D. O.; Malyshkina, I. A.; Vidal, F.; Aubert, P.-H.; Okatova, O. V.; Pavlov, G. M.; Komarova, L. I.; Wandrey, C.; Vygodskii, Y. S. Bis-(Trifluoromethylsulfonyl)Amide Based "Polymeric Ionic Liquids": Synthesis, Purification and Pecularities of Structure-Properties Relationships. *Electrochim. Acta* **2011**, *57*, 74−90.

(40) Penzel, E.; Rieger, J.; Schneider, H. A. The Glass Transition Temperature of Random Copolymers: 1. Experimental Data and the Gordon-Taylor Equation*. *Polymer (Guildf).* **1997**, *38* (2), 325−337.

(41) An, J.; Dèdinaitè, A.; Winnik, F. M.; Qiu, X. P.; Claesson, P. M. Temperature-Dependent Adsorption and Adsorption Hysteresis of a Thermoresponsive Diblock Copolymer. *Langmuir* **2014**, *30* (15), 4333−4341.

(42) Suarez, P. A. Z.; Einloft, S.; Dullius, J. E. L.; De Souza, R. F.; Dupont, J. Synthesis and Physical-Chemical Properties of Ionic Liquids Based on 1- n-Butyl-3-Methylimidazolium Cation. *J. Chim. Phys. Physico-Chimie Biol.* **1998**, *95* (7), 1626−1639.

(43) Chen, S.; Vijayaraghavan, R.; Macfarlane, D. R.; Izgorodina, E. I. Ab Initio Prediction of Proton NMR Chemical Shifts in Imidazolium Ionic Liquids. *J. Phys. Chem. B* **2013**, *117*, 3186−3197.

(44) Atuanya, C. U.; Edokpia, R. O.; Aigbodion, V. S. The Physio-Mechanical Properties of Recycled Low Density Polyethylene (RLDPE)/Bean Pod Ash Particulate Composites. *Results Phys.* **2014**, *4*, 88−95.

(45) Mohapatra, A. K.; Mohanty, S.; Nayak, S. K. Dynamic Mechanical and Thermal Properties of Polylactide-Layered Silicate Nanocomposites. *J. Thermoplast. Compos. Mater.* **2014**, *27* (5), 699−716.

(46) Onuoha, C.; Onyemaobi, O. O.; Anyakwo, C. N.; Onuegbu, G. C. Effect Of Filler Loading And Particle Size On The Mechanical Properties Of Periwinkle Shell-Filled Recycled Polypropylene Composites. *Am. J. Eng. Res.* **2017**, *6* (4), 72−79.

(47) Unal, H.; Mimaroglu, A. A. Influence of Filler Addition on the Mechanical Properties of Nylon-6 Polymer. *J. Reinf. Plast. Compos.* **2004**, *23* (5), 461−469.

(48) Qin, H.; Zhang, S.; Zhao, C.; Feng, M.; Yang, M.; Shu, Z.; Yang, S. Thermal Stability and Flammability of Polypropylene/Montmorillonite Composites. *Polym. Degrad. Stab.* **2004**, *85* (2), 807−813.

(49) Beyer, G. Nanocomposites: A New Class of Flame Retardants for Polymers. *Plast. Addit. Compd.* **2002**, *4* (10), 22−28.

(50) Chen, S.; Lu, X.; Zhang, Z.; Wang, T.; Pan, F. Preparation and Characterization of Poly(Methyl Methacrylate)/Reactive Montmorillonite Nanocomposites. *Polym. Compos.* **2016**, *37*, 2396.

(51) Lee, B. L.; Nielsen, L. E. Temperature Dependence of the Dynamic Mechanical Properties of Filled Polymers. *J. Polym. Sci. Polym. Phys. Ed* **1977**, *15* (4), 683−692.

(52) Ratna, D.; Manoj, N. R.; Varley, R.; Singh Raman, R. K.; Simon, G. P. Clay-Reinforced Epoxy Nanocomposites. *Polym. Int.* **2003**, *52* (9), 1403−1407.